JOURNAL OF GEOPHYSICAL RESEARCH, VOL. 103, NO. B5, PAGES 10,091–10,102, MAY 10, 1998

Fine structure of the 410-km discontinuity

Tim Melbourne and Don Helmberger

Seismological Laboratory, California Institute of Technology

Abstract. The April 14, 1995, earthquake in western Texas (M_w 5.7) produced a strong topside reflection off the 410-km discontinuity which was recorded on a multitude of seismic arrays throughout the southwestern United States. Data from 394 vertical short-period and 24 broadband instruments provide dense coverage of this event from distances of 11° to 19° and provide a detailed look at the subcontinental 410-km structure. The salient features of this data set are (1) the strong dependence on wavelength of the 410-km triplication range, (2) the uniform amplitude ratio of the direct P and reflected P_{410} phases on both short-period and broadband recordings throughout the triplication, and (3) the abrupt termination of the short-period P_{410} phase at 13.3°. These features are best modeled by a composite discontinuity in which a sharp velocity jump of 3% is overlain by a linear velocity jump of 3.5% spread over 14 km. The interference of energy turning in the diffuse and sharp portions of this discontinuity structure reproduces both the long- and short-period triplication range and the step-like behavior of the P_{410} short-period amplitude, which cannot be reproduced with either a simple linearly diffuse or a purely sharp discontinuity. This composite structure produces a triplication range which depends on source frequency and has an apparent depth which depends on observation frequency. Additionally, this is the structure expected from mineralogical arguments for the α to β olivine phase transition.

1. Introduction

The fine structure of upper mantle discontinuities provides basic constraints on chemical and dynamical models of the mantle. Premier among seismic imaging of these discontinuities is identifying the magnitude, sharpness (radial thickness), and topography (radial variability) associated with the velocity jump. The 410-km discontinuity (hereafter referred to as the 410) is generally seismically inferred to have a P velocity change in the vicinity of 5-6 % caused by the olivine α to β transition [*Neele,* 1996; *Vidale et al.,* 1995; *Ringwood,* 1969], but the sharpness and extent of topography have remained less clear. Because the wavelength of body phases typically used to study the discontinuities is of the order of the length scale of the discontinuity itself, any conclusive seismic estimation of the fine structure of the 410 is made difficult by the apparent transition impedance and thickness potentially being as much a function of source spectral content as actual structure [*Burdick and Helmberger,* 1978; *Helffrich and Bina,* 1994]. Reported thicknesses vary by up to a factor of 10, from 35 km under the central Eurasian craton [*Priestley et al.,* 1994] to 2-4 km under oceanic spreading centers in the Indian Ocean [*Benz and Vidale,* 1993]. However, based on unequivocal 1-Hz underside reflections at near-normal incidence and localized topside reflections exhibiting the triplication range of a sharp discontinuity, there has arisen a consensus that the 410 must be, at least locally, < 5 km thick [*Neele,* 1996; *Nakanishi,* 1988; *Benz and Vidale,* 1993].

The pressing difficulty with this estimate is that a sharp 410 conflicts with numerous studies of the equilibrium thermodynamic behavior of a primarily olivine mantle chemistry. For any reasonable mantle composition [*Anderson,* 1989], the $\alpha - \beta$ transition is expected to occur over a few tens of kilometers in the vicinity of 400 km depth, and as improved laboratory results converge, so too does the robustness of this estimate [*Bina and Wood,* 1987; *Katsura and Ito,* 1989]. Besides actual chemical layering in the upper mantle, the seismic conclusion of a sharp jump appears incompatible with anything other than a pure end-member olivine phase transition. Various mechanisms have been proposed to resolve this conflict, including a nonequilibrium, propagating phase transition [*Solomatov and Stevenson,* 1994] or a 410 composed of both transforming olivine and chemical differentiation across the discontinuity [*Anderson,* 1989], but verification of any of these theories depends on identifying or constraining topography on the 410, which also remains unclear. *Revenaugh and Jordan [1991]* found anticorrelated 410 and 670 km topography on the basis of mul-

Paper number 98JB00164.
0148-0227/98/98JB-00164$09.00

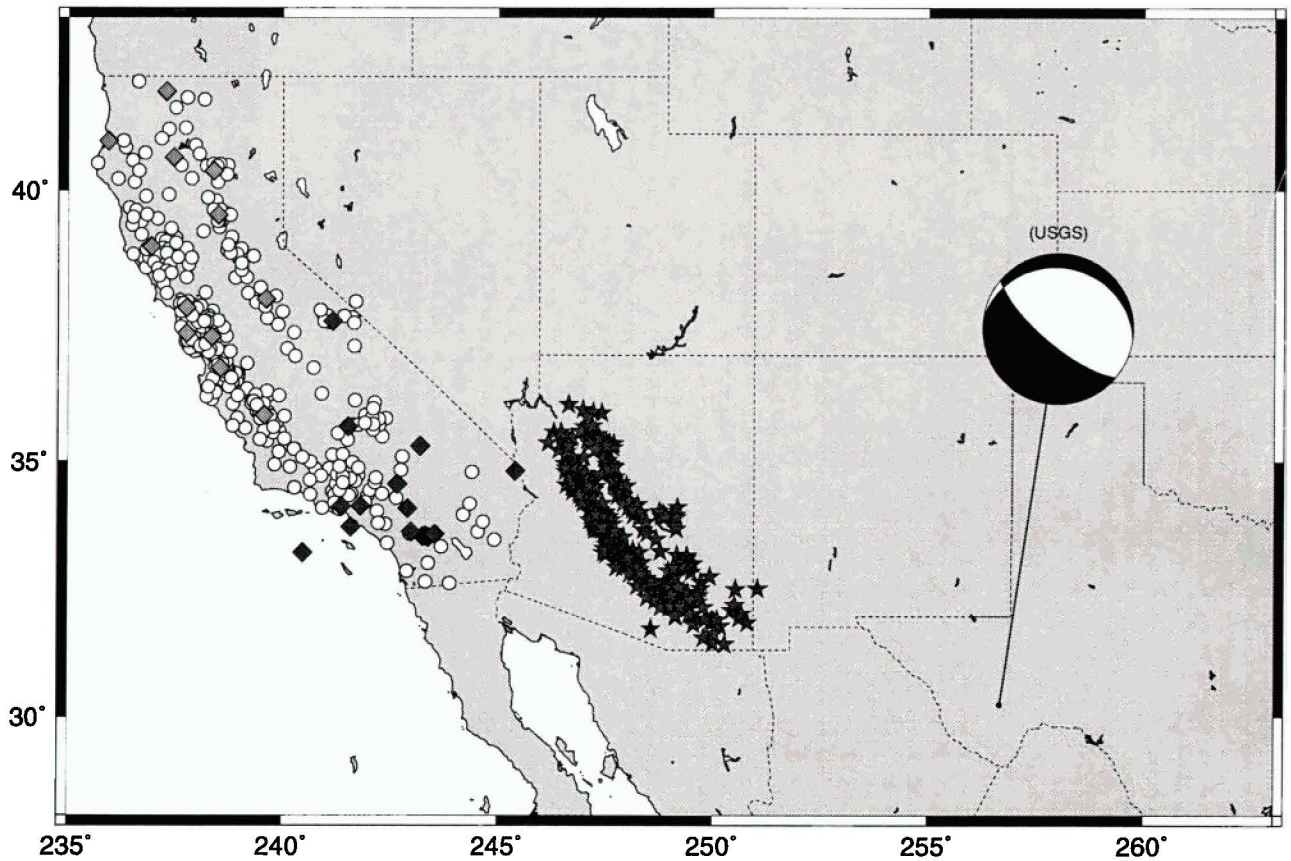

Figure 1. The data set recording the April 14, 1995 west Texas earthquake (M_l 5.7, (30.24, -103.32, 15 km)) contains 394 vertical short-period recordings from the U.S. Geological Survey, Berkeley and California Institute of Technology arrays (open circles) and 28 broadband recordings (diamonds) of which 24 are used in this study. The 410 km discontinuity bounce points for all stations are shown as stars.

tiple *ScS* bounces, whereas more recent studies have found slightly positive to no correlation, as inferred from *P* to *SV* conversions and long-period *SS* precursors [*Shearer,* 1993; *Flanagan and Shearer,* 1998]. From laboratory experiments and thermodynamic calculations, it is expected on the basis of Clapeyron slope magnitudes that the 410-km discontinuity should have more topography than the 670-km discontinuity [*Bina and Helffrich,* 1994], but seismically the opposite has been found [*Shearer,* 1991; *Flanagan and Shearer,* 1998]. In light of thermodynamic arguments for a more diffuse 410 structure, the difficulties introduced by wavelength dependent visibility, the lack of consensus regarding topography on the 410, and the fact that nearly all robust sharpness estimates have come only from oceanic settings, it is premature to conclude that the 410 is globally sharp.

In this paper we analyze a strong topside 410 reflection produced by the April 14, 1995 event in western Texas, an event which produced a rare sampling of 410 structure through a continental corridor. We present evidence that the 410-km discontinuity under the southwestern United States is probably not completely sharp. It is best modeled as a composite structure containing a sharp *P* velocity jump of 3% overlain by a gradational 3.5% transition spread over 14 km. Although there is ample thermodynamic evidence as to why the 410 might assume this type of structure, we reach this conclusion on purely seismological grounds by showing that a composite structure of this specific type is required to reproduce the triplication range and amplitude behavior found in the data and that these features cannot be well modeled by either a simple sharp or linearly diffuse 410. We discuss in detail the mechanism by which such a composite structure reproduces the data, as well as factors unrelated to the 410 structure which might conspire to produce the data set from which our conclusion is drawn, and why we believe alternate explanations of this data are less likely. Finally, we show how this class of composite discontinuities produces an unstable triplication range which depends on earthquake source spectrum.

2. Data

We utilized 394 short-period traces from the combined arrays of the Southern and Northern California Seismic Networks and 24 broadband records from the

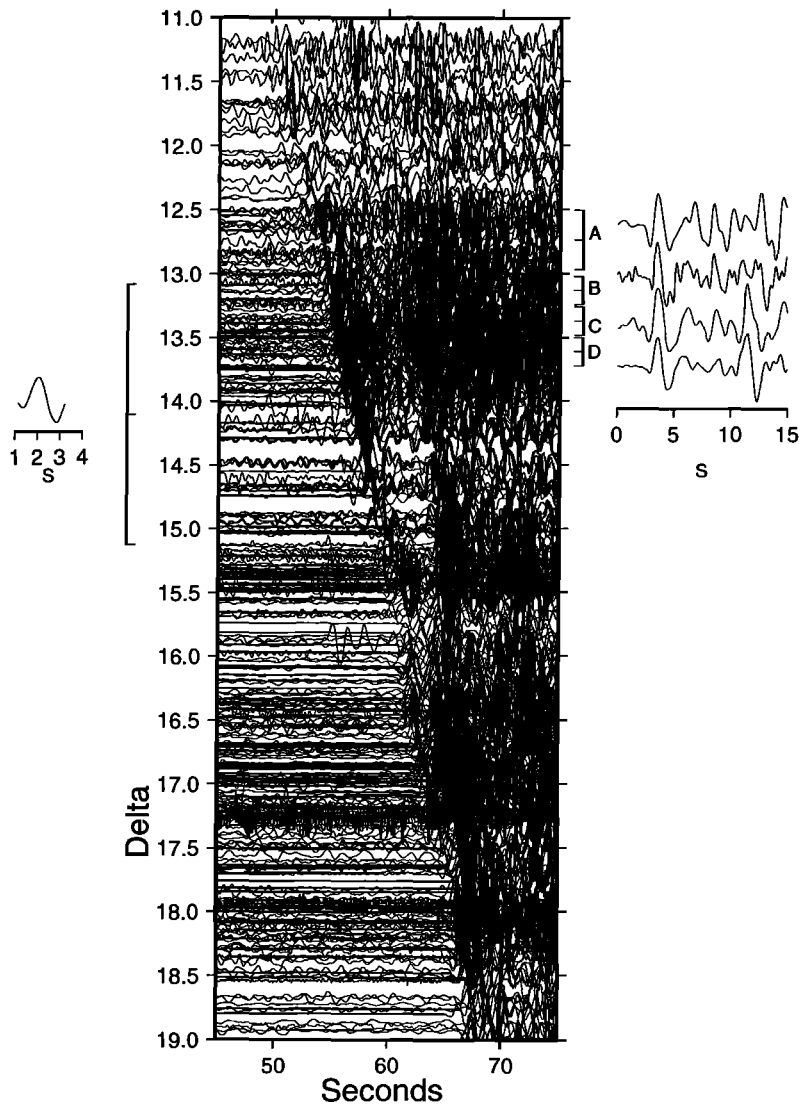

Figure 2. Short-period vertical data plotted with reduction velocity of 10.5 km/s. The 394 traces shown in this array are 1-Hz lowpass filtered and normalized to the maximum amplitude in the window shown. The 410 reflection is clearly visible out to near 13°, where it rapidly disappears. This amplitude decrease is a primary constraint in modeling this data set. To the right of the array are the stacks of the data enclosed in the brackets (see text). To the left is the source time function used in generating synthetics; this consists of the stack of the 82 recordings between 13° and 15°.

seismic arrays operated by Caltech, University of California, Lawrence Livermore National Laboratory and IRIS which recorded the April 14, 1995 Texas event. The source-receiver geometry comprises ray paths with azimuths varying 24° from stations in southern and northern California. This geometry produces a variable bounce point ranging northwest through Arizona (Figure 1). The earthquake occurred along a normal fault with one conjugate plane having strike and dip of 308° and 37° NE [*U.S. Geological Survey,* 1995], placing the west coast short-period array well away from the radiation nodes, with the southernmost stations (those nearest the source and most diagnostic of 410 structure) approaching the radiative maximum. As the critical distance of the upper mantle model T7 [*Burdick and Helmberger,* 1978] is near 14°, most of the focus of this study is on the precritical phase arriving closer than 14°.

To investigate the frequency dependence of 410 reflectivity, we present the short-period data after 1-Hz low-pass filtering (Figure 2) and the broadband data after convolution with a Wood-Anderson long-period (WALP) response (Figure 3). The convolution provides a convenient spectral separation with which to identify the frequency dependence of 410 triplication range. Unless otherwise indicated, each trace in all record sections is normalized to the maximum amplitude in the time window shown. This serves to illustrate the relative

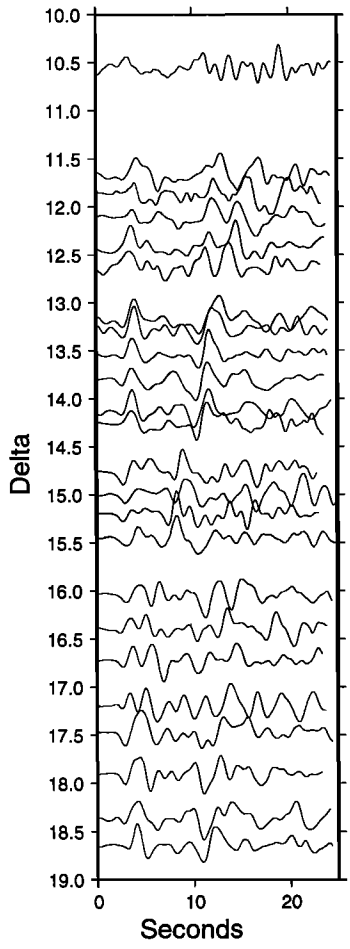

Figure 3. Wood-Anderson convolved broadband recordings. The P_{410} phase is visible out to 11.5°, or 2° farther back than on the corresponding short-period data. This is indicative of the short-period triplication range being controlled by fine structure to which the longer period energy is insensitive.

amplitude of the direct P and 410-reflected arrivals, a fundamental diagnostic of this study. We choose not to analyze absolute amplitudes directly because of the strong dependence on the near-surface receiver structure. Figures 2 and 3 therefore do not show the decay of absolute amplitude with distance or local site amplification effects, however, and cast the P_{410} amplitude in terms of the direct P amplitude, which may be experiencing greater attenuation.

In the long-period record sections (Figure 3), it is straightforward to follow the 410 phase back to 11.6° by tracing the phase with constant slowness inward from 14°, where P_{410} is easily identified. At 12.6° an additional arrival emerges roughly 4 s before P_{410} and is traceable to 10° but is not easily mistaken for the 410 arrival. This precursor is also observed in the stacks of the short-period array data (see below), where it displays a similar moveout to that of the long-period seen here. Since the apparent velocity of the phase is much slower than apparent 410 velocity and the phase shows long-period amplitudes which rapidly decrease with distance, it is most likely the tail end of the crustal wave-guided phase P_{nl} and is therefore unrelated to 410 structure. However, it does appear to interfere with the 410 arrival at ranges between 14° and 16° in that there is a discernible phase shift in P_{410} through this range where the phases come together. Toward 16° the amplitude of P_{nl} appears to be sufficiently small to not perturb the P_{410} phase while near 14° P_{nl} does contribute. At still closer distances diagnostic of 410 structure (12°-14°), the precursor is sufficiently ahead of the P_{410} arrival that interference between the two phases is not an issue. The longer period energy is not particularly sensitive to fine structure of the 410-km discontinuity, and so these data are primarily useful for constraining the total velocity jump across composite 410 structures.

The more diagnostic short-period data are plotted with time reduced at 10.5 s/deg (Figure 2). The 410 phase is plainly visible emerging from the direct P at about 17° and by 14° is about 7 s behind the direct P. A simple estimation by eye suggests that a coherent arrival is visible to a distance of at least 13.5° but not much beyond 13.0°, where there does not appear to be coherent energy above the background noise level. Thus the short-period reflection appears to stay strong until it disappears into the noise over roughly half a degree in range. This rapid amplitude loss provides a fundamental constraint in modeling the 410 reflectivity characteristics.

Because the short-period triplication range is highly sensitive to and diagnostic of 410 structure, it is crucial to tightly constrain the exact range of the P_{410} short-period arrival and its behavior over the range through which it is seen. To that effect, it is useful to stack the data after binning it into segments sufficiently short that the predicted moveout of the P_{410} phase is lower than the intrinsic scatter in P_{410} arrival times. P_{410} coherence can be further improved by aligning each trace to the direct P first motion; this effectively removes the static delays associated with propagation through the receiver-side crust. Because the vertical short-period array employs instruments with substantially different gain factors, each trace is normalized by the maximum amplitude in the stack window before being stacked; this essentially avoids a stack weighted in favor of instruments with higher gain factors.

Owing to the abundance of data between 12.5° and 13.75° and the fact that this end of the triplication branch is diagnostic of discontinuity structure, we divide this region into four bins. The P-aligned, stacked traces are shown in Figure 2 alongside the main record section. Stack A contains 18 traces between 12.5° and 13.0°; stack B contains 15 between 13.0° and 13.25°; stack C contains 17 between 13.25° and 13.5°, and stack D contains 22 traces between 13.5° and 13.75°. Stacks C and D essentially duplicate what can be clearly seen by eye in the unstacked data; the direct P and reflected P_{410} phases dominate the stack and have comparable

magnitudes. The spectrum of both arrivals is broadened due to the scatter in the large number of waveforms in the stack, but stacks with a smaller number of traces in this range reproduce the higher frequency (as well as dominating amplitude) of the arrivals seen in the unstacked data. Neither stack A nor B show a P_{410} arrival clearly discernible above the noise. Particularly striking is the rapid disappearance of P_{410} between stacks C and B; in the former stack, it is the largest arrival, while in the latter there is no positive-swing P_{410} energy visible above the noise despite the two traces having an average separation of only 28 km. The observable downswing in stack B is most likely the vestigial P_{410} phase with a much lower amplitude. Stack A shows neither a strong P arrival nor a P_{410} phase where it should be observed and has a high coda amplitude relative to direct P. This is most likely due to shadowing of direct P from the mantle low-velocity zone [*LeFevre and Helmberger,* 1989] and crustal reverberations; the gradual lessening of direct P amplitude is also observed in the unstacked data in Figure 2. However, since the 410 phase is less affected by lid structure it would still appear in (if not dominate) the stack if indeed energy were returning from the 410 at this range and the lack of a strong direct P phase in stack A would not preclude the observation of P_{410} . There is some hint of an arrival approximately 1.5 s behind where one would expect the P_{410} phase to be arriving in stack A, but the amplitude of this arrival is not much above the coda, unlike in stacks C and D. One can also observe the P_{410} precursor observed in the long-period data and discussed above; because of the distinctly slower moveout and decreasing amplitude, we believe this is the crustal phase P_{nl}. Given the questionable P_{410} signal on stack B, only the late and noise-saturated hint on stack A, and that the P_{410} arrival is not observable past 13.2° in the unstacked data, a primary constraint in modeling 410 reflectivity therefore is that the P_{410} arrival should not be strong at distances closer than 13.2°.

It is instructive to point out how different the Texas short-period P_{410} behavior is from other samples of topside reflections which have been used to infer a sharp 410, particularly the numerous Gulf of California events recorded on west coast networks. When it is seen, these events show a P_{410} arrival as far in as 10° which exhibits a gradual amplitude decay with closer distances, rendering them suitable for modeling with a sharp 410 [*Neele,* 1996; *Walck,* 1984]. The abrupt P_{410} termination shown in the Texas data, however, and the discrepancy of over 3° in the short-period triplication range between this and Baja events are highly suggestive of a P_{410} structure which is not necessarily sharp and displays regional variation.

3. Synthetics

From a modeling standpoint, the key features to reproduce are the frequency dependence of the triplication range, the constant P_{410}/P amplitude ratio, and the abrupt short-period cutoff at 13.3°. The point of the synthetics is not to match every crustal reverberation associated with the source, which contains P, pP, sP, etc., but rather to model the reflective characteristics of the 410-km discontinuity by reproducing the basic behavior of the data. We use generalized ray theory [*Helmberger,* 1983] to calculate synthetics for a host of one-dimensional velocity structures based on a modified version of the model T7 [*Burdick and Helmberger,* 1978] (Figure 4a), which was derived from Californian earthquakes recorded across the United States, including stations in Texas. This model adequately fits the differential travel times of the P and 410 reflected phases, although it should be noted that the "410-km" discontinuity actually occurs at 393 km depth in the original model. Since the fine structure of the discontinuity affects triplication range much more strongly than its absolute depth, we do not perturb the absolute depth of the "410" in this model and but continue to refer to the discontinuity as the "410" since that depth appears by recent estimations to be its rough average depth [*Shearer,* 1991, 1993]. The Cagniard-de Hoop formalism includes density and shear structure only through their influence on the coefficients of reflection and transmission. The waveforms presented in this paper are therefore much more sensitive to the P velocity structure than to density or shear structure [*Gilbert and Helmberger,* 1972).

The source time function used in the synthetics is shown in Figure 2; it consists of the first 2.4 s of the 82 short-period waveforms from 13.5 to 15.5 lined up on the P arrival and stacked. While this source has a slightly longer-period spectrum due to the stacking, the slight source red shift will not seriously bias the reflectivity results for linear velocity models and is found to give substantially the same results as individual traces for the composite (nonlinear) velocity models.

Owing to the precedent set by other studies which have shown the 410 to be sharp, it is appropriate to first evaluate the suitability of models containing a sharp 410. We then gradually increase the thickness of the 410 discontinuity to explore the suitability of linearly diffuse structures. Physically, for the same incidence angle and frequency of energy, the effect of thickening the discontinuity is equivalent to lowering the relative impedance at that frequency across the discontinuity. Since the apparent impedance scales roughly with wavelength for discontinuity thicknesses comparable to the wavelength of the incident energy, increasing the discontinuity thickness preferentially lowers the short-period reflectivity relative to the longer period energy. Figures 5a-5c show short-period synthetic record sections for the three linear discontinuity structures shown in Figure 4b, which have thicknesses of 0, 10, and 20 km. It is evident in these profiles how the thickness of the transition controls the die-off rate of the P_{410} amplitude. The sharp model is clearly inappropriate for the

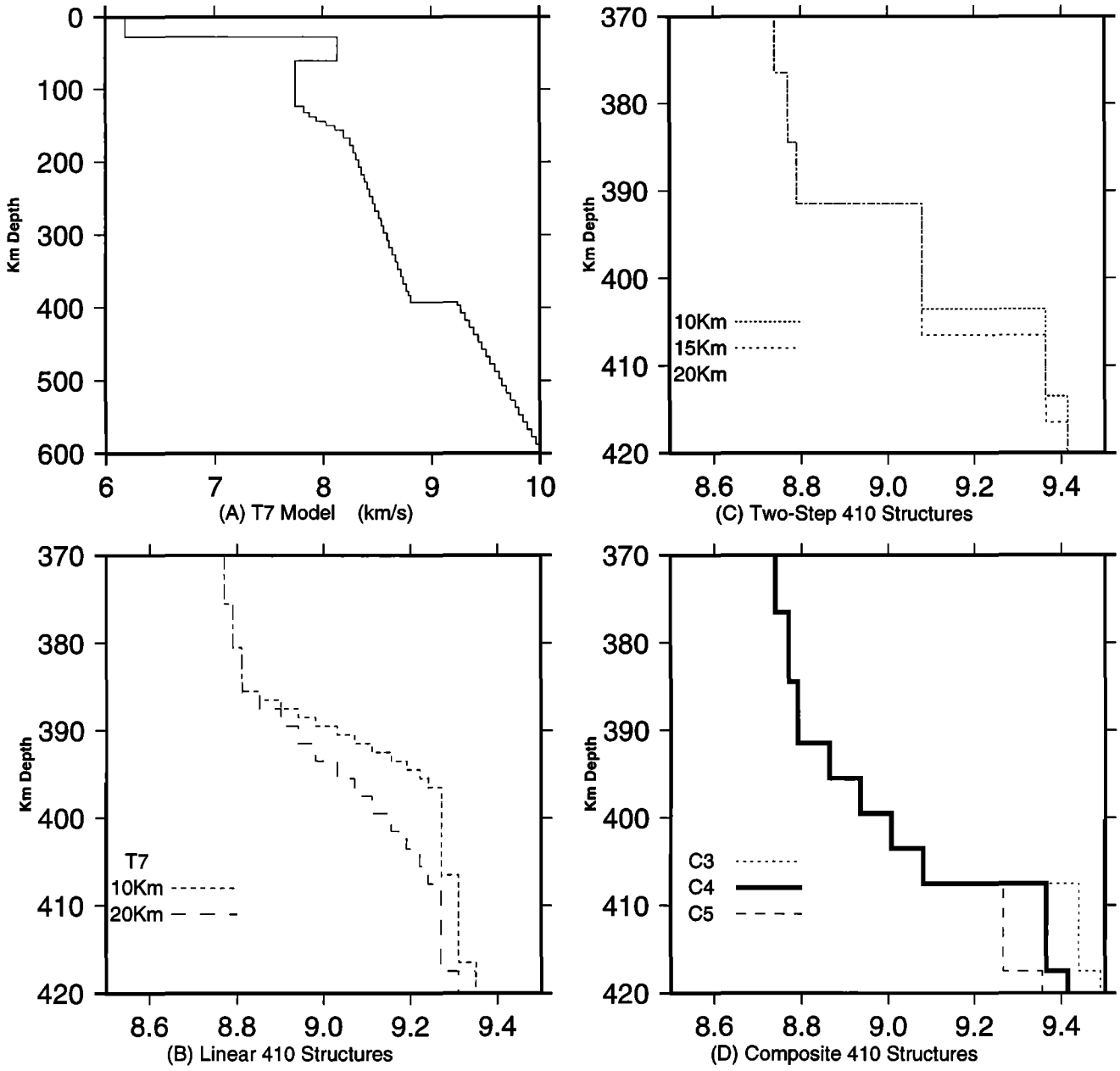

Figure 4. (a) The upper mantle P velocity model T7, derived for California events recorded across the western United States, including stations in Texas. (b) Linear 410-km discontinuity gradients with a 5.5% velocity jump. (c) Double 410 structures. (d) Composite 410 structures consisting of a gradient overlying a sharp offset. The preferred model is labeled C4. Short-period record sections for the models shown in Figures 4b, 4c, and 4d are shown in Figures 5, 7, and 8, respectively. Long-period synthetics appropriate for Figure 3 appear in Figure 6.

Texas data; the synthetic P_{410} phase on short record section is strong back to 11°, contrary to the data.

Taken alone, the frequency dependence of the Texas data triplication range can be reproduced with a diffuse discontinuity of 6% spread over roughly 20 km; the uncertainty in the thickness is based on the criteria by which one judges exactly where on the short-period synthetics the decaying P_{410} phase would no longer be visible above background noise. By setting some detection criteria, a frequency dependent 3° triplication discrepancy could be reproduced with a diffuse model. As is readily seen in Figures 6a and 6b, the long-period triplication range is much less modified by the discontinuity thickness than is the short-period triplication range, allowing one to identify a discontinuity thickness which preferentially limits the short-period triplication range over that of the long-period. The drawback with the linear models of Figure 4b is that none can produce the step-like behavior of the Texas P_{410} amplitude, where the reflected phase has amplitudes comparable to or

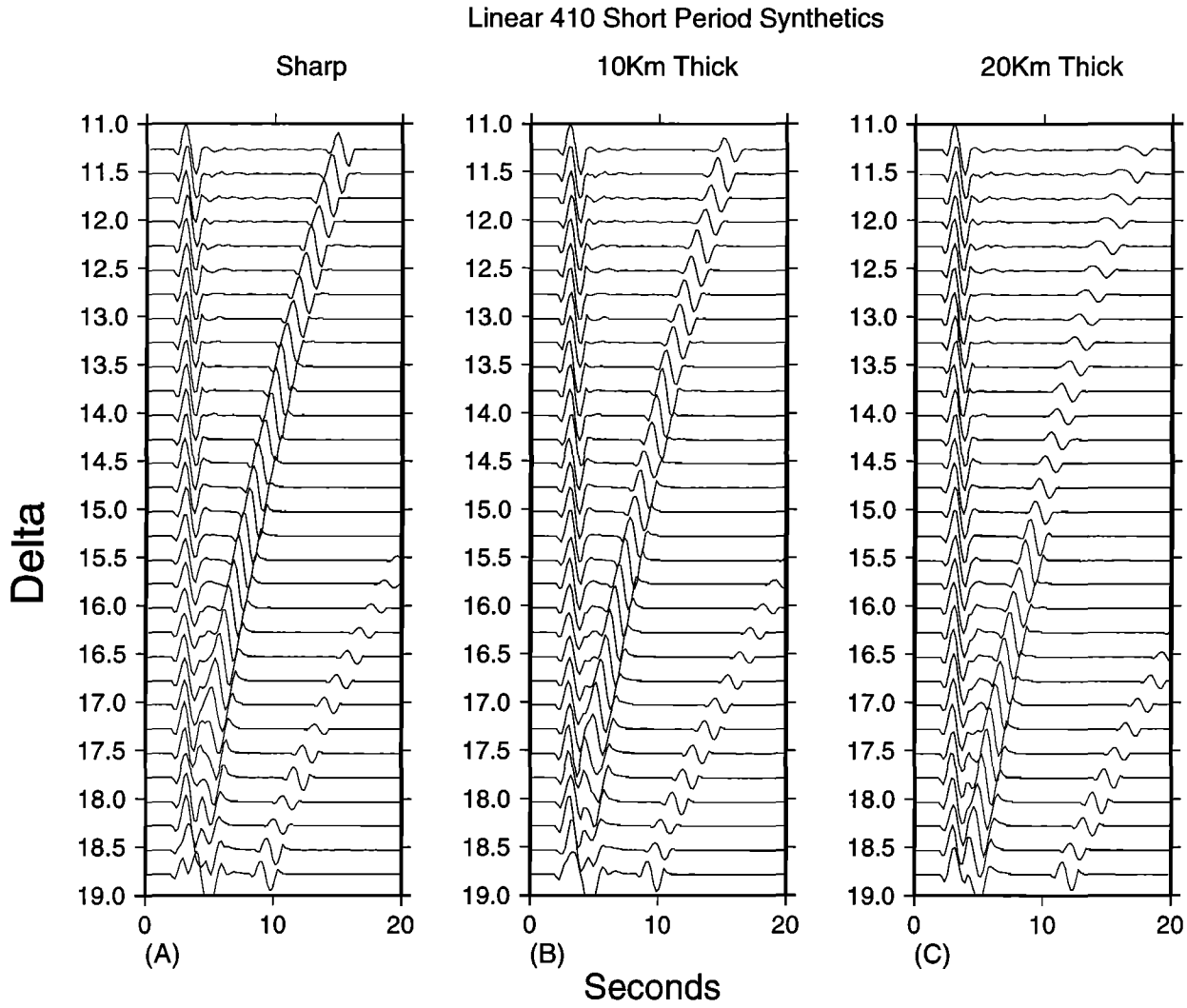

Figure 5. Short-period synthetics for linear 410 gradients. (a) A sharp offset causes the 410 reflected phase to appear strongly as far back as 11°, which is clearly inappropriate for the Texas data. Increasing the thickness to (b) 10 km or (c) 20 km lowers the overall short-period impedance preferentially over the long-period (Figure 6) but cannot produce the very rapid cutoff of P_{410} amplitude seen in the data.

greater than that of the direct P throughout the range where P_{410} appears. Instead, the synthetics for any linearly diffuse structure show a gradual amplitude decay with range relative to direct P but cannot produce an abrupt P_{410} termination. The class of linear discontinuities (particularly sharp ones) is suitable for some studies of the Gulf of California events but is inadequate for the Texas data.

A nonlinear decay of P_{410} amplitude with distance can be produced by introducing fine structure into the discontinuity, which allows energy reflected from discontinuity substructures to interfere. The type of interference depends on the wavelength, angle of incidence, and physical dimensions of the 410 substructures. The reflection of high incidence angle (greater source-receiver distance) energy interferes constructively, essentially because energy traversing different 410 substructures has closer travel times at larger distances. As the source-receiver distance lessens and the separate substructure travel times increasingly differ, the two energy packets (containing the same source function) separate in time, causing a transition to destructive interference. This effect is capable of producing rapid decrease of the P_{410} amplitude over very short distances. Therefore, to find a structure which can reproduce the Texas short-period triplication range and amplitude means to identify the class of discontinuity substructures whose interference is constructive throughout most of the triplication range (thereby maintaining a strong, nondecaying P_{410} arrival) but which turns destructive near 13.2° (thereby reproducing the abrupt P_{410} termination identified in the data).

We explored a variety of 410 substructures before narrowing plausible models down to two simple classes be-

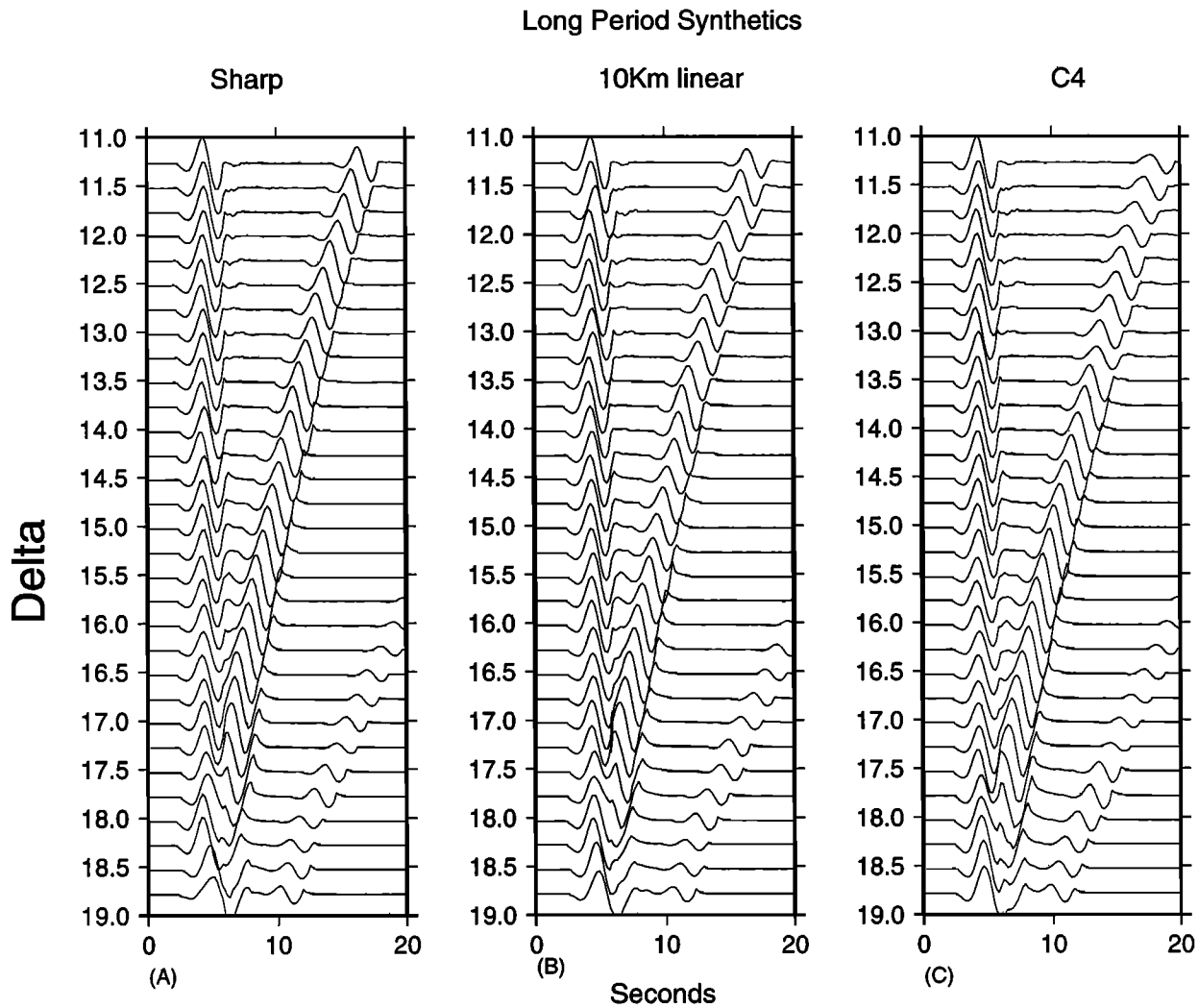

Figure 6. Long-period synthetics for (a) a sharp 410; (b) a 10-km thick linear gradient, and (c) our preferred composite model C4 (Figure 4d). The long-period energy averages over discontinuity fine structure and therefore has a much more stable triplication range which depends primarily on the net jump across the discontinuity. Therefore it is primarily of use in quantifying total velocity jump across the 410.

tween which we feel the data have the resolving power to distinguish. These include double, sharp discontinuities and different permutations of partly diffuse, partly sharp substructures. The double discontinuities were explored by varying the spacing between and velocity change across the jumps, while in the second class of models, different transition thicknesses and velocity contrasts across sharp jumps were tested. Figures 4c and 4d show the most seismically plausible discontinuity structures for the double-jump and diffuse-sharp substructures, respectively, and their corresponding short-period profiles are found in Figure 7 and Figure 8.

The class of structures containing two distinct steps (Figure 4c) produces the transition to destructive interference at a distance which depends more on the spacing between the two jumps then the actual velocity contrast across the jump. With a separation of 20 km (Figure 7a) the P_{410} amplitude starts to drop off around 14.75° and progressively broadens its shape until it splits into a double arrival near 13.5°. Inward of 13.5°, the arrival is clearly split and near 13° has roughly half the amplitude of direct P but rebounds slightly inwards of 12.5°. A 15 km separation (Figure 7b) produces nearly the same profile except the P_{410} broadening begins a degree closer in distance (13.75°) and phase splits apart at 12.75° instead of 13.75°. Progressively moving the double discontinuity closer together (Figure 7c) causes the discontinuity to appear as a single step and the triplication approaches that of a sharp 410. Therefore we can discard double 410 structures that have spacing less than 10 km, as these produce a triplication range extending too far inward.

While this class of two-step discontinuities can produce a 35% decrease in P_{410} amplitude relative to direct

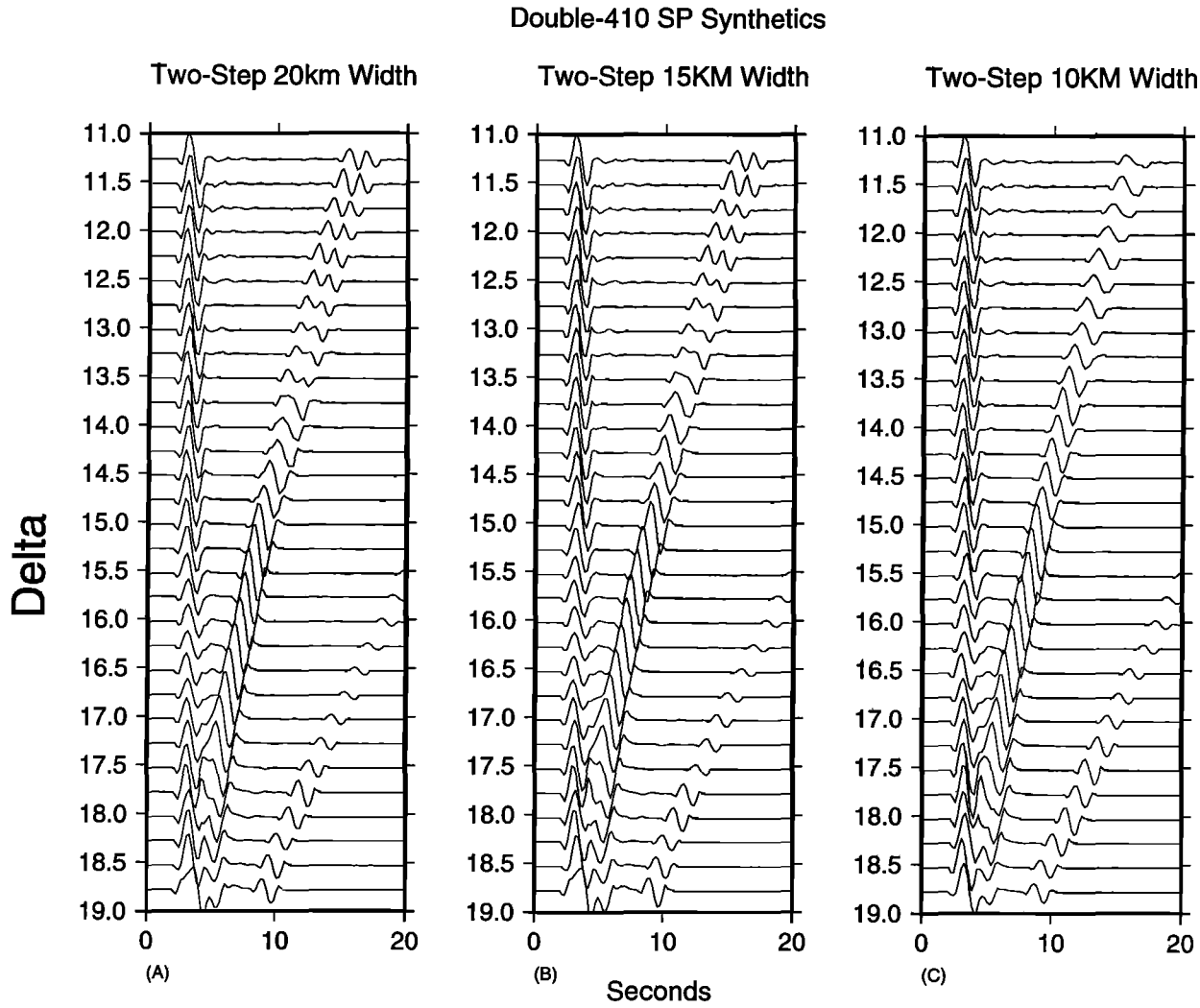

Figure 7. Short-period synthetics with 20, 15, and 10 km thicknesses corresponding to Figure 4c. These models can produce rapid decay of P_{410} , with an onset controlled by the spacing between the velocity jumps. However, these models produce a broadening and splitting of the P_{410} phase not observed in the data.

P over a relatively narrow range (0.5°) with the onset determined by the substep spacing, the spectral broadening of P_{410} is not observed in either the stacked data or in observations of individual waveforms. Nor is there any sign of P_{410} splitting in the data, although energy with this amplitude might be difficult to observe despite its coherence. Increasing or decreasing the magnitude of the either one of the two jumps to more than a cumulative total of about 6% is not viable because both the long- and short-period P_{410} phases become too large at distances near 14°-15°, where both P and P_{410} amplitudes are readily ascertainable. For these reasons we rule out a double 410 structure.

The second class of composite models contain combinations of linearly diffuse and sharp offsets. The most viable models are those in which a sharp substructure is overlain by a velocity gradient. We find through experimentation that the interference phenomenon described above is much less pronounced for structures which have a sharp offset overlying a gradient. We explore the discontinuity model space by adjusting the percentage jump across each substructure and the thickness of the diffuse portion, keeping the total jump over the whole discontinuity near 6% in accordance with the amplitude constraints provided by the data at further distances. Increasing the jump across the sharp portion of the discontinuity serves to extend the triplication range and lessen the overall effect of the interference (Figures 8a-8c), as does thinning the diffuse portion of the nonsharp substructure. In contrast, lowering the sharp offset and thickening the diffuse part both decreases the triplication range and increases the interference such that the P_{410} amplitude decrease behaves much less linearly. Given these trade-offs, our preferred model is shown in Figure 4d (labeled C4), which consists of a gradient of 3.5% spread over 14 km directly overlying an

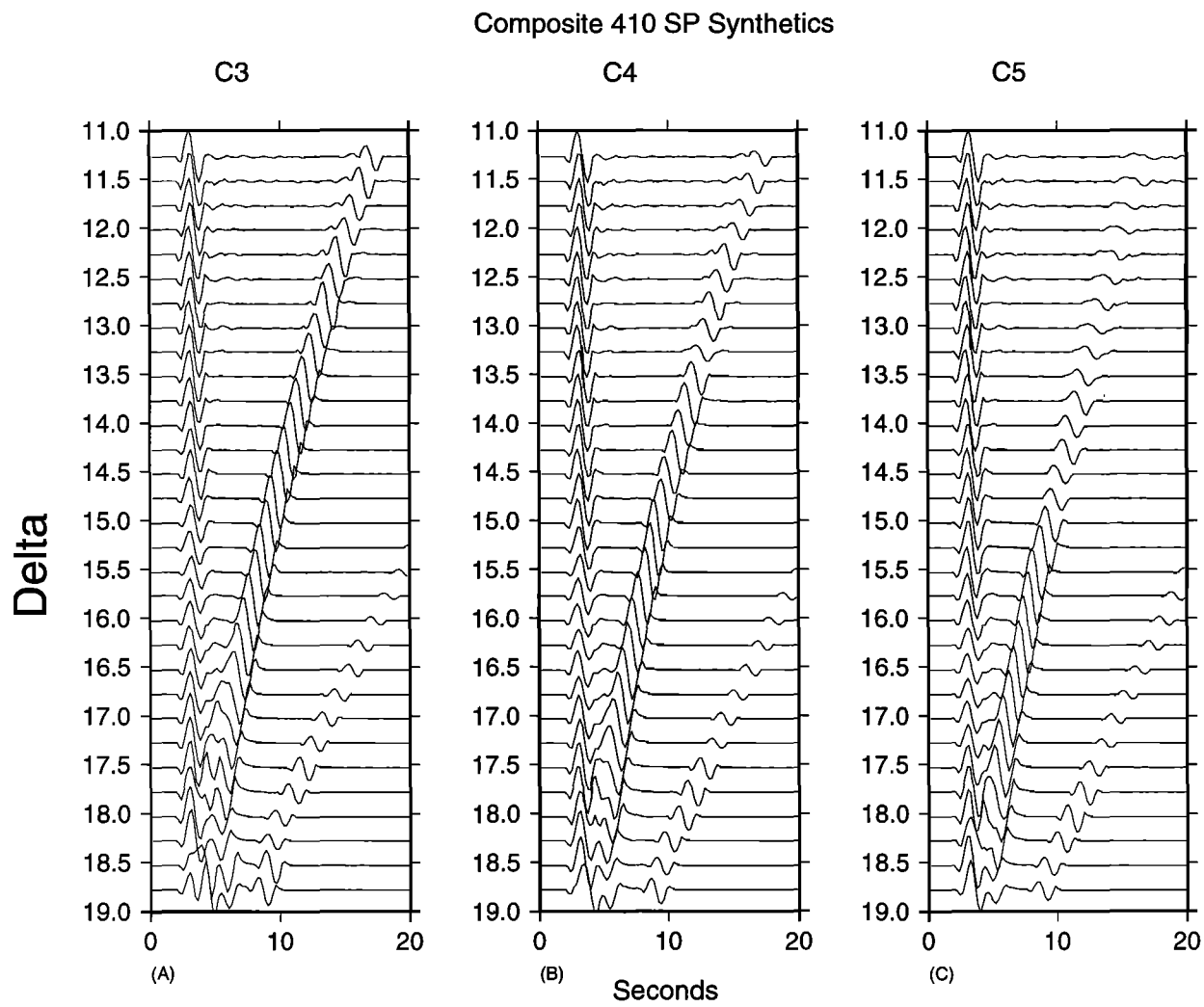

Figure 8. Short-period synthetics for composite discontinuity models consisting of a fixed gradient with a variable sharp step (see Figure 4d). The gradient dimensions were found by trial and error to maximize the interference of energy turning in this portion of the model with energy returning from the sharp region of the 410. The best fit to the data is achieved by (C4), which contains a 3% velocity jump over 15 km. This produces a 56% decrease of P_{410}/P amplitudes ratio over 0.5° and maintains a strong P_{410} amplitude at further distances.

additional sharp discontinuity of 3%. The short-period synthetics for this model are shown in Figure 8b. This model produces a 46% loss of P_{410} amplitude relative to direct P over 0.25° and 56% over 0.5°, and additionally does not produce the strong splitting or spectral broadening of the double-discontinuity models. There is a slight rebound of the amplitude near 12.75° but only by about 10%. Intriguingly, this rebound occurs at the same distance as the stack A which shows the hint of P_{410} reemergence, while the lowest synthetic amplitude at 13.25° corresponds in distance to the stack B which has no P_{410} arrival. Furthermore, at and beyond 13.5°, the synthetic P_{410} has nearly constant amplitude relative to direct P. This model therefore reproduces what we identify to be the most important aspects of the Texas short-period data set and is unquestionably more appropriate than a sharp or linearly diffuse 410-km discontinuity structure. The long-period synthetics appropriate for this model are shown in Figure 6c.

4. Interpretation

The composite model advocated in this study inherently predicts a highly frequency dependent triplication whose range and P_{410} amplitude depend not only on the spectral band of observation but the source time function as well. Via the interference phenomenon described above, two earthquakes with comparable source-receiver ray paths, magnitudes, and mechanisms but different sources would show different triplications despite sampling the same region along the 410-km discontinuity. This source dependence might explain the variable visibility of topside 410 reflections; in one of the most complete studies, *Walck* [1984] found observ-

able P_{410} arrivals in roughly half of the Gulf of California events recorded in Pasadena which sampled similar regions of the 410-km discontinuity. This structure also implicitly generates an ambiguous depth and reflection coefficient which depends on the frequency of observed energy. At longer periods the discontinuity will appear shallower and with a greater net velocity jump because energy is effectively turned by both the diffuse and sharp portions of the structure, whereas shorter-period energy (1 Hz) will preferentially sample only the sharper portion located 10-15 km deeper than the top of the diffuse portion [*Burdick and Helmberger,* 1978; *Helffrich and Bina,* 1994].

Although our analysis does not allow us to distinguish between different petrologic models, a 410-km discontinuity structure of the type advocated here could be produced by either a single component or multicomponent phase transition. In the former, our type of composite 410 phase change is theoretically expected from equilibrium thermodynamic calculations of the $\alpha - \beta$ yield profiles. These show that most of the transformation occurs in a narrow interval near the boundary of the phase loop [*Helffrich and Wood,* 1996; *Stixrude,* 1997], effectively producing a gradient which progressively steepens into a sharp offset. In the latter, the $\alpha-\beta$ olivine phase change superimposed on the broader pyroxene transitions could produce a composite velocity discontinuity marked by linear gradients and sharp offsets [*Anderson,* 1989]. In either of these cases, strong regional variation in 410 triplication behavior is expected given the strong dependence on temperature and chemistry of such a composite discontinuity.

Since the sharp portion of this study's composite structure will always reflect short-period energy, it is not inconsistent with previous studies which have inferred a sharp 410 under oceanic spreading centers [*Walck,* 1984; *Nakanishi,* 1988; *Neele,* 1996], the central Indian Ocean [*Benz and Vidale,* 1993], and Basin and Range [*Vidale et al.,* 1995], particularly since the *P'P'* precursor observations do not provide discontinuity reflection coefficients. The 410-km discontinuity in the majority of previous studies underlies oceanic environments, and there is a body of evidence suggesting that the thermal and chemical differences between oceans and continental cratons extend into the transition zone [*Gossler and Kind,* 1996, *Polet and Anderson,* 1995; *Jordan,* 1975; *Sipkin and Jordan,* 1976], although a consensus on this subject has not yet been achieved [*Flanagan and Shearer,* 1998]. *Gossler and Kind* [1996] find a positive correlation of differential travel times between *SS* precursors and continents and oceans, from which they infer that the subcontinental transition zone is on average 14 km thicker than suboceanic. The opposite sign of the Clapeyron slopes for the phase changes usually associated with the 410- and 660-km discontinuities [*Helffrich and Bina,* 1994] allows this result to be most easily explained by cooler subcontinental transition zone temperatures of on average 100 K. Regional variation on a much shorter lateral scale length has also been documented by Dueker et al. [1997], as well as in high resolution regional tomography models [*Humphreys and Dueker,* 1994]. Given that the 410 bounce points of this study lie within a continental corridor adjacent to the stable (and presumably cool) Colorado Plateau and that the only other study of comparable resolution to this one found a 35 km thick 410 transition beneath Eurasia [*Priestley et al.,* 1994], there is adequate reason to think that subcontinental 410 structure should differ in its overall form from suboceanic environments.

5. Discussion and Conclusions

Perhaps the largest unknown in our model formulation is our inability to quantitatively assess the potential impact on the P_{410}/P amplitude ratio of differential attenuation along the two paths under the tectonically active western United States. Systematically greater attenuation of direct P caused by relatively lower Q along shallower paths would keep the recorded P_{410}/P ratio artificially high throughout the array and could potentially mask a linear drop-off of P_{410} amplitude. However, such attenuation would not produce the abrupt P_{410} cutoff, which is the primary constraint in modeling the data. Therefore the ultimate effect of not modeling attenuation would be a misappraisal of the total velocity change across a composite 410 but would not alter the result that such a composite structure is required to produce the abrupt termination of P_{410}.

The mantle low-velocity zone (LVZ) could also have a significant impact on the P_{410}/P amplitude ratio on both a regional and local scale. Profiles of explosion data from Nevada Test Site recorded in west Texas indicates that P emergence from the shadow zone occurs near 12° [*Helmberger,* 1973], thus causing any diffracted arrivals detected here to be lowered in frequency and amplitude. We argue that the P_{410}/P ratio drops off quickly with decreasing distance; therefore, if the shadow zone is heavily impacting the ratio by lowering the P amplitude then the P_{410} amplitude must be decreasing even faster so as to still lower the ratio as observed. Thus the main observational constraint is only bolstered by the regional P interaction with the LVZ.

It is also possible that strong lateral variation in the LVZ is perturbing the P_{410}/P ratio across the array, in particular because energy arriving at closer stations misses the Colorado Plateau, while that arriving at farther stations traverses it. While we cannot rule this possibility out, a fan plot (time versus azimuth) of the same short-period data shows substantially the same behavior of the P_{410}/P ratio as the bounce points move across the margin of the Colorado Plateau, implying that azimuth (and therefore LVZ lateral variation) is not the cause of the ratio decrease and pointing to the 410-km discontinuity as the source of the phenomenon.

Finally, another possible interpretation of the fre-

quency dependence of triplication range seen in the data is that the 410 under the Colorado Plateau is, in fact, sharp but is strongly laterally varying in a two-dimensional sense, causing wavelength dependent defocusing. Given the transitional nature of the surface tectonics, the above arguments for petrologic differences extending into the upper mantle, and *SS* precursor studies which show variable depths of upper mantle discontinuities [*Flanagan and Shearer,* 1997], this is a distinct possibility. However, it is also quantitatively untestable without additional, orthogonal ray paths recorded on arrays with station density comparable to that presented here.

Ultimately, for the data analyzed in this study, the one dimensional, composite model suffices to explain the gross features of both the short- and long-period P_{410} reflection without needing to invoke a more complicated structure. That the model possesses the basic velocity structure expected from petrologic arguments makes it all the more compelling. It is ominous, however, that only the extremely high station density allows identification of this structure and suggests that the true 410 structure can be easily hidden by limitations in either observation density or spectrum.

Acknowledgments: This research was supported by National Science Foundation grant NSF EAR-9316 441 California Institute of Technology, Seismological Laboratory Contribution 6201.

References

Aki, K., and P.G. Richards, *Quantitative Seismology,* vol.1. W. H. Freeman, New York., 1980.

Anderson, D.L, *Theory of the Earth,* Blackwell, Cambridge, Mass., 1989.

Benz, H., and J. Vidale, Sharpness of upper-mantle discontinuities determined from high-frequency reflections, *Nature ,365,* 147-150, 1993.

Bina, C., and G. Helffrich, Phase transition Clapeyron slopes and transition zone seismic discontinuity topography, *J. Geophys. Res., 99* , 15,853-15,860, 1994.

Bina, C., and B. J. Wood, Olivine-spinel transitions: Experimental and thermodynamic constraints and implications for the nature of the 400-km seismic discontinuity, *J. Geophys. Res., 92* , 4853-4866, 1987.

Burdick, L., and D. V. Helmberger, The upper mantle *P* velocity structure of the western United States, *J. Geophys. Res., 83* , 1699-1712, 1987.

Dueker, K. G., and A. F. Sheehan, Mantle discontinuity structure from midpoint stacks of converted *P* waves to *S* waves across the Yellowstone hotspot track, *J. Geophys. Res., 102* , 8313-8327, 1997.

Flanagan, M.P., and P. Shearer, Global mapping of topography on transition zone velocity discontinuities by stacking *SS* precursors, *J. Geophys. Res., 103,* 2673-2692, 1998.

Gilbert, F., and D. Helmberger, Generalized ray theory for a layered sphere, *Geophys. J. R. Astron. Soc., 27* , 57-80, 1972.

Gossler, J., and R. Kind, Seismic evidence for very deep roots of continents, *Earth Planet. Sci. Lett., 138* , 1-13, 1996.

Helffrich, G., and C. R. Bina, Frequency dependence of the visibility and depths of mantle seismic discontinuities, *Geophys. Res. Lett., 21* , 2613-2616, 1994.

Helffrich, G., and B. Wood, 410 km discontinuity sharpness and the form of the olivine alpha-beta phase diagram- resolution of the apparent seismic contradictions, *Geophys. J. Int., 126,* F7-F12, 1996.

Helmberger, D. V., On the structure of the low velocity zone, *Geophys. J. R. Astron. Soc., 34* , 251-263, 1973.

Helmberger, D. V., Theory and applications of synthetic seismograms, in *Earthquakes: Observation, Theory and Interpretation,* edited by H. Kanamori, pp. 173-222, Soc. It. di Fis., Bologna, Italy, 1983.

Humphreys, E. D., and K. Dueker, Physical state of the western U.S. upper mantle, *J. Geophys. Res., 99,* 9635-9650, 1994.

Jordan, T., The continental tectosphere, *Rev. Geophys., 13,* 1-12, 1975.

Katsura, T., and E. Ito, The system $Mg_2SiO_4 - Fe_2SiO_4$ at high pressures and temperatues: Precise determination of stabilities of olivine, modified spinel, and spinel, *J. Geophys. Res., 94,* 15,663-15,670, 1989.

LeFevre, V., and D. Helmberger, Upper mantle *P* velocity structure of the Canadian shield, *J. Geophys. Res., 94,* 17,749-17,765, 1989.

Nakanishi, I., Reflections of *P'P'* from upper mantle discontinuities beneath the mid-Atlantic ridge, *Geophys. J., 93,* 335-346, 1988.

Neele, F., Sharp 400 km discontinuity from *P* reflections, *Geophys. Res. Lett., 23,* 419-422, 1996.

Polet, J., and D. Anderson, Depth extent of cratons as inferred from tomographic studies, *Geology, 23,* 205-208, 1995.

Priestley, K. F., J. Cipar, A. Egorkin, and N. Pavlenkova, Upper-mantle velocity structure beneath the Siberian platform., *Geophys. J. Int., 118,* 369-378, 1994.

Revenaugh, J., and T. Jordan, Mantle layering from *ScS* reverberations, 1, Waveform inversion of zeroth-order reverberations, *J. Geophys. Res., 96,* 19,749-19,762, 1991.

Ringwood, A.E., Phase transformations in the mantle, *Earth Planet. Sci. Lett, 5,*402-422, 1969.

Shearer, P., Constraints on upper mantle discontinuities from observations of long-period reflected and converted phases, *J. Geophys. Res., 96,* 18,147-18,182, 1991.

Shearer, P., Global mapping of upper mantle reflectors from long-period *SS* precursors, *Geophys. J. Int., 115,* 878-904, 1993.

Sipkin, S., and T. Jordan, Lateral heterogeneity of the upper mantle determined from the travel times of multiple *ScS*, *J. Geophys. Res., 81,* 6307-6320, 1976.

Solomatov, V., and D. J. Stevenson, Can sharp seismic discontinuities be caused by non-equilibrium phase transformations?, *Earth Planet. Sci. Lett., 125,* 267-279, 1994.

Stixrude, L., Structure and sharpness of phase-transitions and mantle discontinuities, *J. Geophys. Res., 102,* 14,835-14,852, 1997.

U. S. Geological Survey(USGS), *Preliminary Determination of Epicenters, U. S. Gov. Print. Off.*, Washington, D.C., 1995.

Vidale, J., X. Y. Ding, and S. P. Grand, The 410-km-depth discontinuity: A sharpness estimate from near critical reflections, *Geophys. Res. Lett., 22,* 2557-2560, 1995.

Walck, M., The *P* wave upper mantle structure beneath an active spreading centre: The Gulf of California, *Geophys. J. R. Astron. Soc., 76,* 697-723, 1984.

D. Helmberger and T. Melbourne, Seismological Laboratory, MS252-21, California Institute of Technology, Pasadena, CA 91125. (e-mail: helm@gps.caltech.edu; tim@gps.caltech.edu)

(Received July 1, 1997; revised January 1, 1998; accepted January 12, 1998.)